

Hybrid adaptive feedforward-feedback compensation algorithms for active vibration control systems

Marouane Alma, Ioan Doré Landau, John Jairo Martinez, Tudor-Bogdan Airimîtoaie

Abstract—The paper addresses the problem of simultaneous adaptive feedforward compensation and feedback compensation of vibrations (or noise) when a correlated measurement with the disturbance (an image of the disturbance) is available. The study is carried in the presence of a "positive" mechanical coupling between the compensator system and the measurement of the image of the disturbance, which often occurs in practice. The positive mechanical coupling introduces a coupling between the design of the feedback loop and the stability conditions for the adaptive feedforward compensation. Modifications of the algorithms for adaptive feedforward compensation has to be considered. The new algorithms proposed are analyzed and have been applied to an active vibration control system featuring internal positive mechanical coupling.

Index Terms—active vibration control, adaptive feedforward compensation, RS controller, adaptive control, hybrid feedforward-feedback compensation, parameter estimation

I. INTRODUCTION

Adaptive feedforward for broadband disturbance compensation is widely used when a well correlated signal with the disturbance (image of the disturbance) is available ([3], [4], [8], [14]). However in many systems there is a positive mechanical coupling between the feedforward compensation system and the measurement of the image of the disturbance. This often leads to the instability of the system. Different solutions have been proposed taking into account this coupling (see for example [7], [9], [6]). Analysis of some existing algorithms in this modified context are also available [13]

Combining adaptive feedforward compensation with feedback control has been considered as an issue for further improving the performance of the adaptive feedforward compensation alone. Several references are available, like [2], [12], [5].

One of the solutions given in [2], is to use the feedback controller for reducing the effect of periodic disturbances and feedforward compensation to reject broadband disturbances. The main drawback of this work is the absence of any stability analysis. In [12], it is stated that using a feedback controller with a good gain margin may improve the stability and performance of the adaptive feedforward compensation, but a detailed analysis is not provided.

The objectives of this paper are

- to analyse the interaction between the feedback loop and the adaptive feedforward compensation.

M. Alma, I.D. Landau, J.J. Martinez, T.B. Airimîtoaie are with the control system department of Gipsa-lab, St martin d'hères, 38402 FRANCE ([marouane.alma, ioan-dore.landau, john-jairo.martinez-molina, Tudor-Bogdan.Airimitoaie]@gipsa-lab.grenoble-inp.fr)

- to develop and analyse recursive algorithms for online estimation and adaptation of the parameters of the feedforward filter compensator for broadband disturbances in the presence of the feedback controller.
- to take into account the internal positive coupling occurring in many AVC and ANC systems.
- to apply the algorithms on an active vibration control system featuring internal positive mechanical coupling.

One of the important observations resulting from the analysis developed in this paper, is that the stability conditions for the adaptive feedforward compensation are highly influenced by the the design of the feedback loop. This interaction is further enhanced when the internal positive coupling is present. The major practical consequence is that the filters used in order to assure the stability conditions for the adaptive feedforward compensation will depend upon the elements of the feedback compensation loop built around the compensation system (called secondary path - see section II).

While the paper is developed in the context of AVC (active vibration control) systems, the results are applicable to ANC systems.

II. AN ACTIVE VIBRATION CONTROL SYSTEM USING AN INERTIAL ACTUATOR

Figures 1 and 2 represent an AVC system using a measurement correlated with the disturbance and an inertial actuator for reducing the residual acceleration. The structure is representative for a number of situations encountered in practice.

The system consists of 5 metallic plates connected by springs. The plates M1 and M3 are equipped with inertial actuators. The one on M1 serves as disturbance generator (inertial actuator 1 in figure 2), the one on M2 serves for disturbance compensation (inertial actuator 2 in figure 2). The system is equipped with a measure of the residual acceleration (on plate M3) and a measure of the image of the disturbance made by an accelerometer posed on plate M1. The path between the disturbance (in this case, generated by the inertial actuator on top of the structure), and the residual acceleration is called the *global primary path*. The path between the measure of the image of the disturbance and the residual acceleration (in open loop) is called the *primary path* and the path between the inertial actuator for compensation and the residual acceleration is called the *secondary path*. When the compensator system is active, the actuator acts upon the residual acceleration, but also upon the measurement of the image of the disturbance (a positive feedback). The measured quantity $\hat{u}(t)$ will be the sum of

The positive feedback coupling is characterized by the asymptotically stable transfer operator:

$$M(q^{-1}) = \frac{B_M(q^{-1})}{A_M(q^{-1})} \quad (7)$$

where:

$$B_M(q^{-1}) = b_1^M q^{-1} + \dots + b_{n_{B_M}}^M q^{-n_{B_M}} = q^{-1} B_M^*(q^{-1}) \quad (8)$$

$$A_M(q^{-1}) = 1 + a_1^M q^{-1} + \dots + a_{n_{A_M}}^M q^{-n_{A_M}} \quad (9)$$

The identified models of the secondary path and of the positive feedback coupling will be denoted \hat{G} and \hat{M} , respectively.

The fixed RS controller K , computed on the basis of model \hat{G} to reject broadband disturbances on the output χ , is characterized by the asymptotically stable transfer function:

$$K(q^{-1}) = \frac{B_K(q^{-1})}{A_K(q^{-1})} \quad (10)$$

where:

$$B_K(q^{-1}) = b_0^K + b_1^K q^{-1} + \dots + b_{n_{B_K}}^K q^{-n_{B_K}} \quad (11)$$

$$A_K(q^{-1}) = 1 + a_1^K q^{-1} + \dots + a_{n_{A_K}}^K q^{-n_{A_K}} \quad (12)$$

The optimal feedforward filter (unknown) is defined by :

$$N(q^{-1}) = \frac{R(q^{-1})}{S(q^{-1})} \quad (13)$$

where:

$$R(q^{-1}) = r_0 + r_1 q^{-1} + \dots + r_{n_R} q^{-n_R} \quad (14)$$

$$S(q^{-1}) = 1 + s_1 q^{-1} + \dots + s_{n_S} q^{-n_S} = 1 + q^{-1} S^*(q^{-1}) \quad (15)$$

The estimated filter is denoted by $\hat{N}(q^{-1})$ or $\hat{N}(\hat{\theta}, q^{-1})$ when it is a linear filter with constant coefficients or $\hat{N}(t, q^{-1})$ during estimation (adaptation) of its parameters.

The input of the feedforward filter is denoted by $\hat{u}(t)$ and it corresponds to the measurement provided by the primary transducer (force or acceleration transducer in AVC or a microphone in ANC). In the absence of the compensation loop (open loop operation) $\hat{u}(t) = d(t)$. The "a posteriori" output of the feedforward filter is denoted by $\hat{y}_1(t+1) = \hat{y}_1(t+1|\hat{\theta}(t+1))$. The "a priori" output of the estimated feedforward filter is given by:

$$\begin{aligned} \hat{y}_1^0(t+1) &= \hat{y}_1(t+1|\hat{\theta}(t)) \\ &= -\hat{S}^*(t, q^{-1})\hat{y}_1(t) + \hat{R}(t, q^{-1})\hat{u}(t+1) \\ &= \hat{\theta}^T(t)\phi(t) = [\hat{\theta}_S^T(t), \hat{\theta}_R^T(t)] \begin{bmatrix} \phi_{\hat{y}_1}(t) \\ \phi_{\hat{u}}(t) \end{bmatrix} \end{aligned} \quad (16)$$

where

$$\hat{\theta}^T(t) = [\hat{s}_1(t) \dots \hat{s}_{n_S}(t), \hat{r}_0(t) \dots \hat{r}_{n_R}(t)] = [\hat{\theta}_S^T(t), \hat{\theta}_R^T(t)] \quad (17)$$

$$\begin{aligned} \phi^T(t) &= [-\hat{y}_1(t) \dots -\hat{y}_1(t-n_S+1), \hat{u}(t+1), \hat{u}(t) \dots \hat{u}(t-n_R+1)] \\ &= [\phi_{\hat{y}_1}^T(t), \phi_{\hat{u}}^T(t)] \end{aligned} \quad (18)$$

and $\hat{y}_1(t)$, $\hat{y}_1(t-1) \dots$ are the "a posteriori" outputs of the feedforward filter generated by:

$$\hat{y}_1(t+1) = \hat{y}_1(t+1|\hat{\theta}(t+1)) = \hat{\theta}^T(t+1)\phi(t) \quad (19)$$

while $\hat{u}(t+1)$, $\hat{u}(t) \dots$ are the measurements provided by the primary transducer².

The control signal applied to the secondary path is given by

$$\hat{y}(t+1) = \hat{y}_1(t+1) - \frac{B_K}{A_K} \chi(t+1) \quad (20)$$

The unmeasurable "a priori" output of the secondary path will be denoted $\hat{z}^0(t+1)$.

$$\hat{z}^0(t+1) = \hat{z}(t+1|\hat{\theta}(t)) = \frac{B_G^*(q^{-1})}{A_G(q^{-1})} \hat{y}(t) \quad (21)$$

The "a posteriori" unmeasurable value of the output of the secondary path is denoted by:

$$\hat{z}(t+1) = \hat{z}(t+1|\hat{\theta}(t+1)) \quad (22)$$

The measured primary signal (called also reference) satisfies the following equation:

$$\hat{u}(t+1) = d(t+1) + \frac{B_M^*(q^{-1})}{A_M(q^{-1})} \hat{y}(t) \quad (23)$$

The measured residual error satisfies the following equation:

$$\chi^0(t+1) = \chi(t+1|\hat{\theta}(t)) = \hat{z}^0(t+1) + x(t+1) \quad (24)$$

The "a priori" adaptation error is:

$$v^0(t+1) = -\chi^0(t+1) = -x(t+1) - \hat{z}^0(t+1) \quad (25)$$

The "a posteriori" adaptation (residual) error (which is computed) will be given by:

$$v(t+1) = v(t+1|\hat{\theta}(t+1)) = -x(t+1) - \hat{z}(t+1) \quad (26)$$

When using an estimated filter \hat{N} with constant parameters: $\hat{y}^0(t) = \hat{y}(t)$, $\hat{z}^0(t) = \hat{z}(t)$ and $v^0(t) = v(t)$.

IV. DEVELOPMENT AND ANALYSIS OF THE ALGORITHMS

The algorithms for adaptive feedforward compensation in presence of RS feedback controller will be developed under the following hypotheses:

- 1) H1 - The signal $d(t)$ is bounded
i.e.

$$|d(t)| \leq \alpha \quad \forall t \quad (0 \leq \alpha < \infty) \quad (27)$$

(which is equivalently to say that $s(t)$ is bounded and $W(q^{-1})$ in figure 3 is asymptotically stable).

- 2) H2 - Perfect matching condition. There exists a filter $N(q^{-1})$ of finite dimension such that³:

$$\frac{N}{(1-NM)}G = -D \quad (28)$$

and the characteristic polynomials:

of the "internal" positive coupling loop

$$P(z^{-1}) = A_M(z^{-1})S(z^{-1}) - B_M(z^{-1})R(z^{-1}) \quad (29)$$

of the closed loop (G-K):

$$P_{cl}(z^{-1}) = A_G(z^{-1})A_K(z^{-1}) + B_G(z^{-1})B_K(z^{-1}) \quad (30)$$

² $\hat{u}(t+1)$ is available before adaptation of parameters starts at $t+1$

³In many cases, the argument q^{-1} or z^{-1} will be dropped out

and the coupled feedforward-feedback loop:

$$P_{fb-ff} = A_M S[A_G A_K + B_G B_K] - B_M R A_K A_G \quad (31)$$

are Hurwitz polynomials.

- 3) H3 - The effect of the measurement noise upon the measured residual error is neglected (deterministic context).

Once the algorithms will be developed under these hypotheses, hypotheses 2 and 3 will be removed and the algorithms will be analyzed in this modified context.

A first step in the development of the algorithms is to establish a relation between the errors on the estimation of the parameters of the feedforward filter and the measured residual acceleration. This is summarized in the following lemma.

Lemma 4.1: *Under hypotheses H1, H2 and H3, for the system described by equations (1) through (26) using a feedforward compensator \hat{N} with constant parameters, one has:*

$$v(t+1) = \frac{A_M(q^{-1})A_G(q^{-1})A_K(q^{-1})G(q^{-1})}{P_{fb-ff}(q^{-1})} [\theta - \hat{\theta}]^T \phi(t) \quad (32)$$

where

$$\theta^T = [s_1, \dots, s_{n_S}, r_0, r_1, \dots, r_{n_R}] = [\theta_S^T, \theta_R^T] \quad (33)$$

is the vector of parameters of the optimal filter N assuring perfect matching

$$\hat{\theta}^T = [\hat{s}_1 \dots \hat{s}_{n_S}, \hat{r}_0 \dots \hat{r}_{n_R}] = [\hat{\theta}_S^T, \hat{\theta}_R^T] \quad (34)$$

is the vector of constant estimated parameters of \hat{N}

$$\begin{aligned} \phi^T(t) &= [-\hat{y}_1(t) \dots -\hat{y}_1(t-n_S+1), \hat{u}(t+1), \hat{u}(t) \dots \hat{u}(t-n_R+1)] \\ &= [\phi_{y_1}^T(t), \phi_u^T(t)] \end{aligned} \quad (35)$$

and $\hat{u}(t+1)$ is given by

$$\hat{u}(t+1) = d(t+1) + \frac{B_M^*(q^{-1})}{A_M(q^{-1})} \hat{y}(t) \quad (36)$$

The proof is given in the Appendix. The results of Lemma 4.1 can be easily particularized for the case without internal positive feedback or without RS feedback controller

Filtering the vector $\phi(t)$ through an asymptotically stable filter $L(q^{-1}) = \frac{B_L}{A_L}$, equation (32) for $\hat{\theta} = \text{constant}$ becomes:

$$v(t+1) = \frac{A_M(q^{-1})A_G(q^{-1})A_K(q^{-1})G(q^{-1})}{P_{fb-ff}(q^{-1})L(q^{-1})} [\theta - \hat{\theta}]^T \phi_f(t) \quad (37)$$

with:

$$\phi_f(t) = L(q^{-1})\phi(t) \quad (38)$$

Equation (37) will be used to develop the adaptation algorithms neglecting for the moment the non-commutativity of the operators when $\hat{\theta}$ is time varying (however an exact algorithm can be derived in such cases - see [11]).

Replacing the fixed estimated parameters by the current estimated parameters, equation (37) becomes the equation of the a-posteriori residual error $v(t+1)$ (which is computed):

$$v(t+1) = \frac{A_M(q^{-1})A_G(q^{-1})A_K(q^{-1})}{P_{fb-ff}(q^{-1})L(q^{-1})} G(q^{-1})[\theta - \hat{\theta}(t+1)]^T \phi_f(t) \quad (39)$$

Equation (39) has the standard form for an a-posteriori adaptation error ([11]), which immediately suggests to use the following parameter adaptation algorithm:

$$\hat{\theta}(t+1) = \hat{\theta}(t) + F(t)\Phi(t)v(t+1); \quad (40)$$

$$v(t+1) = \frac{v^0(t+1)}{1 + \Phi^T(t)F(t)\Phi(t)}; \quad (41)$$

$$F(t+1) = \frac{1}{\lambda_1(t)} \left[F(t) - \frac{F(t)\Phi(t)\Phi^T(t)F(t)}{\lambda_1(t) + \Phi^T(t)F(t)\Phi(t)} \right] \quad (42)$$

$$1 \geq \lambda_1(t) > 0; 0 \leq \lambda_2(t) < 2; F(0) > 0 \quad (43)$$

$$\Phi(t) = \phi_f(t) \quad (44)$$

where $\lambda_1(t)$ and $\lambda_2(t)$ allow to obtain various profiles for the matrix adaptation gain $F(t)$ (see section V and [11]). By taking $\lambda_2(t) \equiv 0$ one gets a constant adaptation gain matrix (and choosing $F = \gamma I$, $\gamma > 0$ one gets a scalar adaptation gain).

Three choices for the filter L will be considered, leading to three different algorithms:

Algorithm I: $L = G$

Algorithm II⁴: $L = \hat{G}$

Algorithm III:

$$L = \frac{\hat{A}_M \hat{A}_G A_K}{\hat{P}_{fb-ff}} \hat{G} \quad (45)$$

where :

$$\hat{P}_{fb-ff} = \hat{A}_M \hat{S} [\hat{A}_G A_K + \hat{B}_G B_K] - \hat{B}_M \hat{R} A_K \hat{A}_G \quad (46)$$

is an estimation of the characteristic polynomial of the coupled feedforward-feedback loop computed on the basis of available estimates of the parameters of the filter \hat{N} .

For the Algorithm III several options for updating \hat{P}_{fb-ff} can be considered:

- Run Algorithm II for a certain time to get estimates of \hat{R} and \hat{S}
- Run a simulation (using the identified models)
- Update \hat{P}_{fb-ff} at each sampling instant or from time to time using Algorithm III (after a short initialization horizon using Algorithm II)

A. Analysis of the Algorithms

For algorithms I, II and III the equation for the a-posteriori adaptation error has the form:

$$v(t+1) = H(q^{-1})[\theta - \hat{\theta}(t+1)]^T \Phi(t) \quad (47)$$

where:

$$H(q^{-1}) = \frac{A_M A_G A_K}{P_{fb-ff} L(q^{-1})} G, \Phi = \phi_f \quad (48)$$

⁴another option is to use $L = \frac{\hat{G}}{1 + \hat{G}K}$

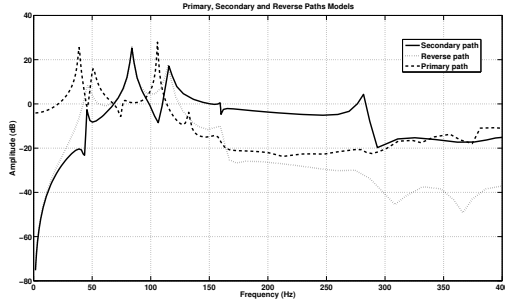


Fig. 4. Frequency characteristics of the primary, secondary and reverse paths

Neglecting the non-commutativity of time varying operators, one has the following result:

Lemma 4.2: Assuming that eq. (47) represents the evolution of the a posteriori adaptation error and that the parameter adaptation algorithm (40) through (44) is used, one has:

$$\lim_{t \rightarrow \infty} v(t+1) = 0 \quad (49)$$

$$\lim_{t \rightarrow \infty} \frac{[v^0(t+1)^2]}{1 + \Phi(t)^T F(t) \Phi(t)} = 0 \quad (50)$$

$$\|\Phi(t)\| \text{ is bounded} \quad (51)$$

$$\lim_{t \rightarrow \infty} v^0(t+1) = 0 \quad (52)$$

for any initial conditions $\hat{\theta}(0), v^0(0), F(0)$.

The proof is similar to that given in [9] for $B_K = 0$ and $A_K = 1$ (absence of the feedback controller) and it is omitted.

V. EXPERIMENTAL RESULTS

A. System identification

A detailed view of the mechanical structure used for the experiments has been given in figure 1.

The excitation signal used to identify the different paths of the system was a PRBS (pseudo-random binary sequence). More details can be found in [9]. The model orders for the secondary path and the reverse path have been estimated to be: $n_{B_G} = 17, n_{A_G} = 15, n_{B_M} = 16, n_{A_M} = 16$. The estimated orders of the model of the primary path are $n_{B_D} = 26, n_{A_D} = 26$. The frequency characteristics of the various paths are shown in figure 4.

B. Design of the feedback controller

The objective of the feedback RS controller K is to reduce the disturbance effect on the output $\chi(t)$ where the secondary path G has enough gain and without using the correlated measurement $u(t)$. To do this, the problem has been formulated as an H_∞ problem by using the appropriate weighting functions.

This minimization problem has been solved using Pole Placement with Sensitivity functions shaping techniques presented in [10],

C. Broadband disturbance rejection

The adaptive feedforward filter structure for most of the experiments has been $n_R = 9, n_S = 10$ (total of 20 parameters) and this complexity does not allow to verify the "perfect matching condition" (not enough parameters). A PRBS excitation on the global primary path will be considered as the disturbance.

For the *adaptive* operation the Algorithms II and III have been used with decreasing adaptation gain ($\lambda_1(t) = 1, \lambda_2(t) = 1$) combined with a *constant trace* adaptation gain [11].

The experiments have been carried out by first applying the disturbance in open loop during 50s and after that closing the loop with the hybrid adaptive feedforward-feedback algorithms. Time domain results obtained in open loop and with hybrid control (using adaptive feedforward compensation algorithm III) on the AVC system are shown in figure 5. The filter for algorithm III has been computed based on the parameter estimates obtained with algorithm II at $t=3600s$ (similar results are obtained if the initialization horizon is of the order of 200 s). The initial trace of the matrix adaptation gain was 10 and the constant trace has been fixed at 0.2.

The variance of the residual force without the feedback con-

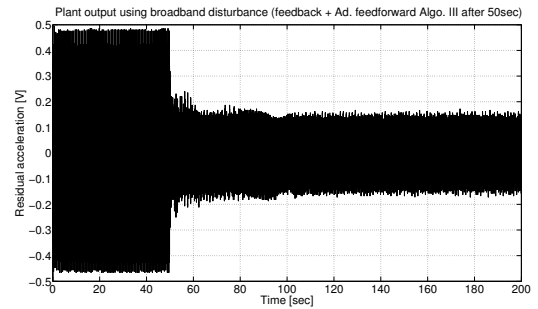


Fig. 5. Real time results obtained with feedback RS controller and adaptive feedforward Algorithm III

troller and feedforward compensator is: $var(\chi(t) = x(t)) = 0.0354$. With the feedback RS controller, the variance is: $var(\chi(t)) = 0.0067$ (14.40dB). Using a model based compensator with an optimal H_∞ feedforward compensator ([1]) and the constant feedback used in the previous experiments, one obtains a variance of the residual acceleration of $var(\chi(t)) = 0.0042$ (18.42dB) (no adaptation capabilities for this two compensation schemes). When in addition to the feedback controller, the adaptive feedforward compensation is active (algorithm III) the variance of the residual acceleration is: $var(\chi(t)) = 0.0033$ (20.53dB). When using only adaptive feedforward compensation (algorithm III) the variance of the residual acceleration is $var(\chi(t)) = 0.0054$ (16.23dB). Clearly, hybrid adaptive feedforward-feedback scheme brings a significant improvement in performance with respect to the other schemes offering in addition adaptation capabilities with respect to the disturbance characteristics or changes in the primary path model.

Figure 6 shows the power spectral densities of the residual acceleration measured on the AVC for the cases discussed

above. The corresponding global attenuations are also given.

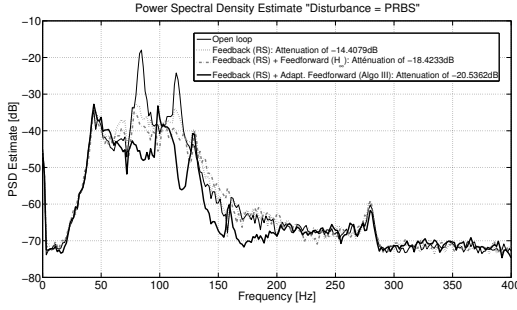


Fig. 6. Power spectral densities of the residual acceleration (Disturbance = PRBS)

VI. CONCLUSIONS

The introduction of a feedback controller on one hand modifies the stability conditions and on the other hand improves significantly the performances of the adaptive feedforward compensation schemes.

VII. APPENDIX- PROOF OF LEMMA 4.1

Under the assumption H2 (perfect matching condition) the output of the primary path can be expressed as:

$$x(t) = -z(t) = -G(q^{-1})y(t) \quad (53)$$

where $y(t)$ is a dummy variable given by:

$$\begin{aligned} y(t+1) &= -S^*(q^{-1})y(t) + R(q^{-1})u(t+1) \\ &= \theta^T \varphi(t) = [\theta_S^T, \theta_R^T] \begin{bmatrix} \varphi_y(t) \\ \varphi_u(t) \end{bmatrix} \end{aligned} \quad (54)$$

and:

$$\theta^T = [s_1, \dots, s_{n_S}, r_0, r_1, \dots, r_{n_R}] = [\theta_S^T, \theta_R^T] \quad (55)$$

$$\begin{aligned} \varphi^T(t) &= [-y(t) \dots -y(t-n_S+1), u(t+1) \dots u(t-n_R+1)] \\ &= [\varphi_y^T(t), \varphi_u^T(t)] \end{aligned} \quad (56)$$

and $u(t)$ is given by:

$$u(t+1) = d(t+1) + \frac{B_M^*(q^{-1})}{A_M(q^{-1})}y(t) \quad (57)$$

For a fixed value of the parameter vector $\hat{\theta}$ characterizing the estimated filter $\hat{N}(q^{-1})$ of same dimension as the optimal filter $N(q^{-1})$, the output of the secondary path can be expressed by (in this case $\hat{z}(t) = \hat{z}^0(t)$ and $\hat{y}(t) = \hat{y}^0(t)$):

$$\hat{z}(t) = G(q^{-1})[\hat{y}(t)] \quad (58)$$

with:

$$\hat{y}(t) = \hat{y}_1(t) + \frac{B_K}{A_K}v(t) \quad (59)$$

where $\hat{y}_1(t+1) = \hat{\theta}^T \phi(t)$. The key observation is that the dummy variable $y(t+1)$ can be expressed as:

$$\begin{aligned} y(t+1) &= \theta^T \phi(t) + \theta^T [\varphi(t) - \phi(t)] \\ &= \theta^T \phi(t) - S^*[y(t) - \hat{y}_1(t)] + R[u(t+1) - \hat{u}(t+1)] \end{aligned} \quad (60)$$

Define the dummy error (for a fixed vector $\hat{\theta}$)

$$\begin{aligned} \varepsilon(t+1) &= y(t+1) - \hat{y}(t+1) \\ &= y(t+1) - \hat{y}_1(t+1) - KG\varepsilon(t+1) \\ &= \frac{1}{1+KG}[y(t+1) - \hat{y}_1(t+1)] \end{aligned} \quad (61)$$

and the residual error becomes:

$$v(t+1) = z(t+1) - \hat{z}(t+1) = G(q^{-1})\varepsilon(t+1) \quad (62)$$

By taking into account the equations (59) and (62), $y(t+1)$ becomes:

$$\begin{aligned} y(t+1) &= \theta^T \phi(t) - S^*[y(t) - \hat{y}(t) + \frac{B_K B_G}{A_K A_G} \varepsilon(t)] \\ &\quad + R[u(t+1) - \hat{u}(t+1)] \end{aligned} \quad (63)$$

It results from (63) by taking into account the expressions of $u(t)$ and $\hat{u}(t)$ given by (57) and (23) (or (36)) that:

$$y(t+1) = \theta^T \phi(t) - [S^*(q^{-1})(1 + \frac{B_K B_G}{A_K A_G}) - \frac{R(q^{-1})B_M^*(q^{-1})}{A_M(q^{-1})}] \varepsilon(t) \quad (64)$$

Using equations (59), (61) and (62), one gets (after passing all terms in ε on the left hand side) equation (32). End of the proof.

REFERENCES

- [1] M. Alma, J.J. Martinez, and I.D. Landau. Design and tuning of h-infinity feedforward compensator for active vibration control system, in presence of feedback controller. Internal report, Gipsa-Lab. INP-Grenoble, 2011.
- [2] R. De Callafon. Active noise control method and apparatus including feedforward and feedback controller, March 2010.
- [3] S.J. Elliott and P.A. Nelson. Active noise control. *Noise / News International*, pages 75–98, June 1994.
- [4] S.J. Elliott and T.J. Sutton. Performance of feedforward and feedback systems for active control. *IEEE Transactions on Speech and Audio Processing*, 4(3):214–223, May 1996.
- [5] E. Esmailzadeh, A. Alasty, and A.R. Ohadi. Hybrid active noise control of a one-dimensional acoustic duct. *Journal of vibration and acoustics*, 124(1):10–18, 2002.
- [6] C.A Jacobson, C.R Johnson, D.C Mc Cormick, and W.A Sethares. Stability of active noise control algorithms. *IEEE Signal Processing letters*, 8(3):74–76, 2001.
- [7] M.S. Kuo and D.R. Morgan. *Active noise control systems- Algorithms and DSP implementation*. Wiley, New York, 1996.
- [8] M.S. Kuo and D.R. Morgan. Active noise control: A tutorial review. *Proceedings of the IEEE*, 87:943–973, 1999.
- [9] I.D. Landau and M. Alma. An adaptive feedforward compensation algorithm for active vibration control. *Proceedings of the 49th IEEE Conference on Decision and Control, Atlanta, USA*, pages 3626–3631, 2010.
- [10] I.D. Landau, J. Langer, D. Rey, and J. Barnier. Robust control of a 360 flexible arm using the combined pole placement/sensitivity function shaping method. *IEEE Transactions on Control Systems Technology*, 4(4):369–383, juillet 1996.
- [11] I.D. Landau, R. Lozano, and M. M'Saad. *Adaptive control*. Springer, London, 1997.
- [12] L.R. Ray, J.A. Solbeck, A.D. Streeter, and R.D. Collier. Hybrid feedforward-feedback active noise reduction for hearing protection and communication. *The Journal of the Acoustical Society of America*, 120(4):2026–2036, 2006.
- [13] A.K. Wang and W. Ren. Convergence analysis of the filtered-u algorithm for active noise control. *Signal Processing*, 73:255–266, 1999.
- [14] J Zeng and R.A de Callafon. Recursive filter estimation for feedforward noise cancellation with acoustic coupling. *Journal of sound and vibration*, 291:1061–1079, 2006.